

CFD Modeling of Multi-fuel Combustion of Coal and Meat and Bone Meal (MBM) in a Cement Rotary Kiln

W. K. Hiromi Ariyaratne, Morten C. Melaen, and Lars-André Tokheim

Abstract—Many cement companies are burning waste-derived fuels in cement kilns due to different advantages. Meat and bone meal (MBM) is such a fuel which gives no net CO₂ emissions to the atmosphere. However, some characteristics of waste-derived fuels can impact the kiln process adversely. In the present study, computational fluid dynamics (CFD) modelling is used to analyze the combustion characteristics when the primary coal energy is partly replaced by MBM. The investigated replacement ratios (by energy) are 10%, 32%, 59% and 90%. Unburnt fuel char can disturb the internal cycles of sulphur, chlorine and alkalis in the cement kiln system and thereby negatively impact the process operation as well as the product quality. A linear correlation between equilibrium gas temperature and fuel replacement ratio was found, but the correlation between overall char burnout and fuel replacement ratio was found to be positively deviated from a linear correlation. The positive deviation increases up to a fuel replacement ratio of 58%. Above this value, the positive deviation starts to drop. Therefore, from a char burnout point of view, a fuel replacement ratio of 58% can be seen as a guiding value for optimum replacement of coal by MBM.

Index Terms—Cement rotary kiln, CFD, fuel char burnout, multi-fuel combustion.

I. INTRODUCTION

The cement manufacturing process is very energy-intensive due to high temperature requirement [1]. Clinkerization (production of clinker) is the most important process that takes place in the kiln system, which basically consists of two combustion units; the precalciner and the rotary kiln. Coal, petroleum coke and other fossil fuels have traditionally been the main fuels burned in the cement kilns. However, these traditional fuels are rather expensive and also contribute to global warming due to high net CO₂ emissions to the atmosphere. Employing energy rich waste as alternative fuels has greatly helped the cement industry to manage its environmental impact and energy costs. Meat and bone meal (MBM), waste tires, waste oils, solvents, plastics, paper, wood, rubber, sewage sludge and refused derived fuels (RDF) are examples of some waste-derived fuels used in cement kilns [2]. Among those fuels, biomass fuels are more attractive since these give no net CO₂ emissions to the atmosphere. It is, however, very important to understand the combustion behaviour of these waste-derived fuels inside the

cement kiln, since some characteristics of those fuels can impact the kiln process adversely, and may also reduce clinker quality, production rate or kiln refractory life [3].

Computational fluid dynamics (CFD) modeling can be an effective and advanced tool to predict the combustion characteristics inside a rotary kiln, and the CFD approach is applied in the current work. Even though many studies have been carried out to model coal combustion in rotary kilns, very few have focused on CFD modeling of waste-derived fuel combustion in cement rotary kilns. Moreover, the modeling studies are limited to only certain types of fuels. Among waste-derived fuels, solid fuel combustion is more complex than gas fuel combustion and more challenging to model.

Abbas, Lockwood and Suhail have developed in-house models to resolve the issues related to alternative fuel and raw material usage in cement plants [4], [5]. A multi-fuel combustion CFD code was developed to take into account any number and combinations of gaseous/liquid and solid fuels [5]. Their publication present combustion characteristics and emissions (temperature, NO and CO) for a wet cement kiln, when coal, natural gas and whole tires (mid-injection) are used in proportions of 75, 3 and 22% of the total thermal input, respectively [5]. However, their paper does not provide comprehensive details about the models and the results.

Recently, a CFD study was carried out by Mtui to investigate the combustion behaviour when different blends of shredded scrap tires and pulverized pine wood are used as fuels in a cement rotary kiln [6]. The substitution ratio was varied from 5 to 20 wt%. Temperature distribution, devolatilization, char conversion and kiln wall heat transfer rates were presented. It was found that up to 20% biomass blends provide improved combustion characteristics compared with combustion of scrap tires alone. The biomass blend was found to increase the flame spreading and penetration, consequently improving the wall heat transfer rate, therefore providing favourable conditions for heat transfer to the cement clinker.

In 2004, ASPEN PLUS process modeling tool was used by a research group who predicted 5-10 % higher combustion air demand when primary energy was replaced by meat and bone meal and sewage sludge [7]. However, process modeling tools can provide only limited information about fluid dynamics, complex heat and mass transfer processes and the solid/gas interactions inside the kiln [3].

Meat and bone meal is one of the waste-derived fuels used in cement kilns, particularly quite widely in Western Europe. This fuel is prepared by grinding and sterilizing slaughter house wastes [8]. This is a pure biofuel and hence more attractive as an environmentally friendly fuel. In a previous

Manuscript received October 20, 2015; revised December 15, 2015.

W. K. Hiromi Ariyaratne and Lars-André Tokheim are with Telemark University College, Department of Process, Energy & Environmental Technology, Faculty of Technology, Kjølnes Ring 56, Post box 203, N-3901 Porsgrunn, Norway (e-mail: hiromi.ariyaratne@hit.no, Lars.A.Tokheim@hit.no).

Morten C. Melaen is with Telemark University College, Faculty of Technology, Kjølnes Ring 56, Post box 203, N-3901 Porsgrunn, Norway (e-mail: morten.c.melaen@hit.no).

modeling study carried out by the authors of the current study, it was found that the kiln gas flow rate is higher and the kiln gas temperature is lower for MBM than for several other solid waste-derived fuels, when replacing 100% of the coal energy in the cement rotary kiln [3], [8]. A full-scale cement kiln test also demonstrated the negative effects of burning high amounts of MBM [9]. Moreover, the authors of the current study used CFD to carry out simulations of MBM combustion. The first publication mainly discusses the impacts of fuel characteristics on combustion properties such as gas temperature, devolatilization, char burnout [10], while the second paper investigates the effect of fuel feeding position and fuel particle size on the combustion characteristics [3]. Both publications discuss the effects of replacing 100% of the coal by MBM, i.e. single-fuel combustion. In general, it was found that MBM combustion gives lower equilibrium gas temperature and also poorer char burnout. Even though the poor char burnout does not explain more than 0.6 % of the temperature drop, the existence of fuel char at the kiln inlet (also referred to as the kiln end in this paper) can have a negative effect on the process by disturbing the internal cycles of sulphur, chlorine and alkalis in the kiln system [11]. This might lead to the conclusion that coal replacement with alternative fuels should be avoided. However, replacement ratios up to a certain value may be acceptable based on positive interactions between coal and alternative fuels when certain mixtures are applied. For example, one might expect a non-linear relationship between replacement ratio and char burnout since the latter is non-linearly dependent on particle temperature, which in turn is a function of gas temperature. Therefore, certain mixtures of coal and MBM may give significantly better burnout than could be expected from anticipating a linear correlation. This hypothesis is tested in the present study.

Steady state three-dimensional simulations were carried out using the commercial CFD software ANSYS FLUENT, version 13.0. Process parameters, kiln and burner dimensions were taken from a full-scale cement plant in Norway which produces around 3400 tons of clinker per day. Coal and MBM are the fuels considered for the simulations. The effect of gravity is included, however the solid charge, clinker reactions and kiln rotation are neglected.

II. MODEL DESCRIPTION

Basic models used are briefly presented here. One may refer to [3] for more details about the models.

A. Gas Phase

The steady state continuity equation and momentum equation for three directions are given in (1) and (2), respectively.

$$\nabla \cdot (\rho \vec{v}) = S_m \quad (1)$$

$$\nabla \cdot (\rho \vec{v} \vec{v}) = -\nabla P + \nabla \cdot (\bar{\tau}) + \rho \vec{g} + \vec{F} \quad (2)$$

$\bar{\tau}$ is the stress tensor given by,

$$\bar{\tau} = \mu_{eff} \left[(\nabla \vec{v} + \nabla \vec{v}^T) - \frac{2}{3} \nabla \cdot \vec{v} I \right]. \quad (3)$$

μ_{eff} models the effect of the molecular and turbulent viscosity.

The Re-Normalisation Group (RNG) k- ϵ model is used for turbulence. The equations for k and ϵ are as follows.

$$\frac{\partial}{\partial x_i} (\rho k u_i) = \frac{\partial}{\partial x_i} \left[\alpha_k \mu_{eff} \frac{\partial k}{\partial x_i} \right] + G_k + G_b - \rho \epsilon \quad (4)$$

$$\frac{\partial}{\partial x_i} (\rho \epsilon u_i) = \frac{\partial}{\partial x_i} \left[\alpha_\epsilon \mu_{eff} \frac{\partial \epsilon}{\partial x_i} \right] + C_{1\epsilon} \frac{\epsilon}{k} (G_k + C_{3\epsilon} G_b) - C_{2\epsilon} \rho \frac{\epsilon^2}{k} \quad (5)$$

G_k represents the generation of turbulence kinetic energy due to the mean velocity gradients and G_b represents the generation of turbulence kinetic energy due to buoyancy. The energy equation can be written in vector notation as follows.

$$\nabla \cdot (\vec{v}(\rho E + P)) = \nabla \cdot (k_{eff} \nabla T - \sum_i h_i \vec{j}_i + (\bar{\tau}_{eff} \cdot \vec{v})) + S_h \quad (6)$$

$$E = h - \frac{P}{\rho} + \frac{v^2}{2} \quad (7)$$

Gas-phase gray radiation is modelled using the P1 model (8) [12]. Particulate effects from char, ash and soot on radiation were not included. The radiation diffusion coefficient is calculated by (9).

$$\nabla \cdot (\Gamma \nabla G) = aG - 4an^2 \sigma T^4 \quad (8)$$

$$\Gamma = \frac{1}{(3(a+\sigma_s) - c\sigma_s)} \quad (9)$$

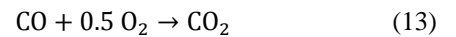
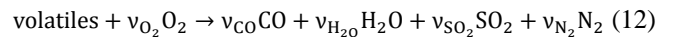
The radiation flux (10) can be substituted into the energy equation (6) to account for heat sources or sinks due to radiation.

$$-\nabla \cdot q_r = \nabla \cdot (\Gamma \nabla G) \quad (10)$$

The species transport equation (11) is solved to obtain the species mass fractions.

$$\nabla \cdot (\rho \vec{v} Y_i) = -\nabla \cdot \vec{j}_i + R_i + S_i \quad (11)$$

The homogeneous reactions are defined by the eddy-dissipation model proposed by Magnussen and Hjertager [13]. The combustion of volatiles is treated as two-step global reactions, as given below.



B. Particle Phase

The Lagrangian discrete phase model is selected for the present study. The equations solved for the particulate phase are presented by (14) and (15).

$$\frac{d\vec{u}_p}{dt} = F_D (\vec{v} - \vec{u}_p) + \frac{\vec{g}(\rho_p - \rho)}{\rho_p} \quad (14)$$

$$\frac{d\vec{x}}{dt} = \vec{u}_p \quad (15)$$

$F_D (\vec{v} - \vec{u}_p)$ is the drag force per unit particle mass. For the calculation of drag coefficient, coal and MBM particles are considered as smooth and spherical in shape.

In the present study, the stochastic tracking approach with ten independent trackings is used to determine the turbulence effect of the fluid phase on the particle dispersions. The turbulent eddies produced by the particles are, however, not accounted in the turbulence model.

The single kinetic rate devolatilization model, and the kinetic/diffusion limited rate model are used for devolatilization and char combustion modeling, respectively [12]. The particle size is assumed to remain constant in char combustion model.

III. COMPUTATIONAL DETAILS

A. Geometry and Grid Generation

A three-dimensional kiln was created in Gambit version 2.4.6. Modifications made for the real rotary kiln (Fig. 1) are briefly pointed out here and one may refer to [3] for further details of the geometry.

- 2) Modified dimensions and shapes were used for the burner inlets compared with the real system (Fig. 1). The 16 swirl air inlets and 20 jet air inlets were converted to annulus sections (in Fig. 1 (left), only a few of swirl air inlets and jet air inlets are shown). However, care was taken to use a flow area that would conserve not only mass but also momentum.
- 3) Liquid hazardous waste and waste oil inlets were discarded (Fig. 1) because those fuels were not applied in this study.
- 4) The solid fuel inlet was moved into the center (Fig. 1).
- 5) The kiln and the burner are taken as horizontal.

Also the mesh was generated in Gambit (Fig. 2). A Cooper type mesh which consists of hexahedral elements is used. The total number of cells in the mesh is 335907. The computational time was around 20-25 days for a run depending on the conditions, when a 2.60 GHz Intel® core™ i7-3720QM processor and 16GB installed memory were used.

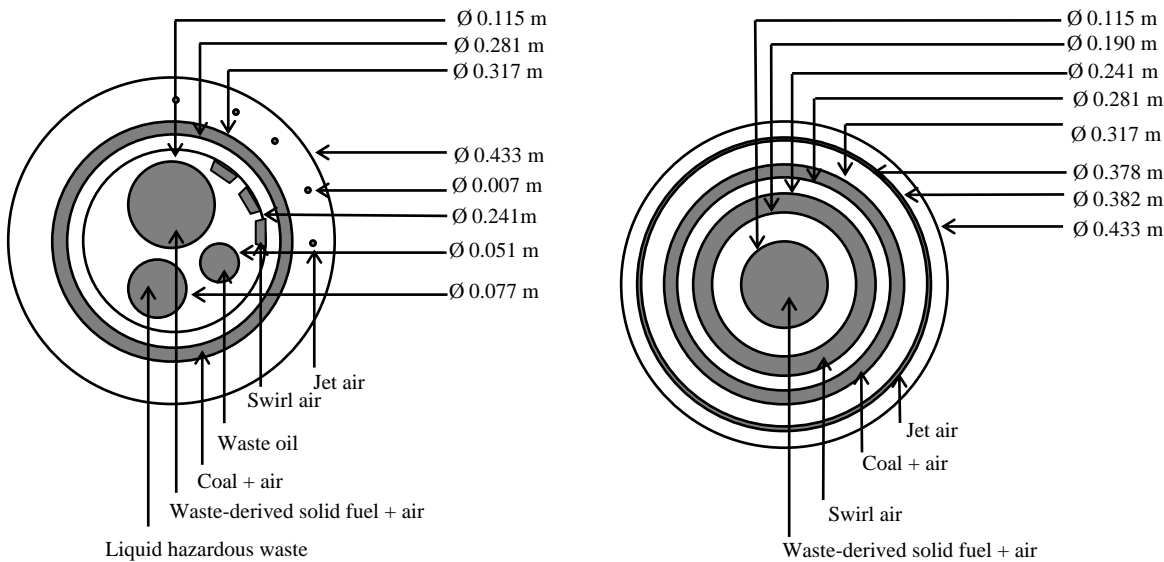


Fig. 1. The dimensions of real (left) and simplified (right) kiln burner [3].

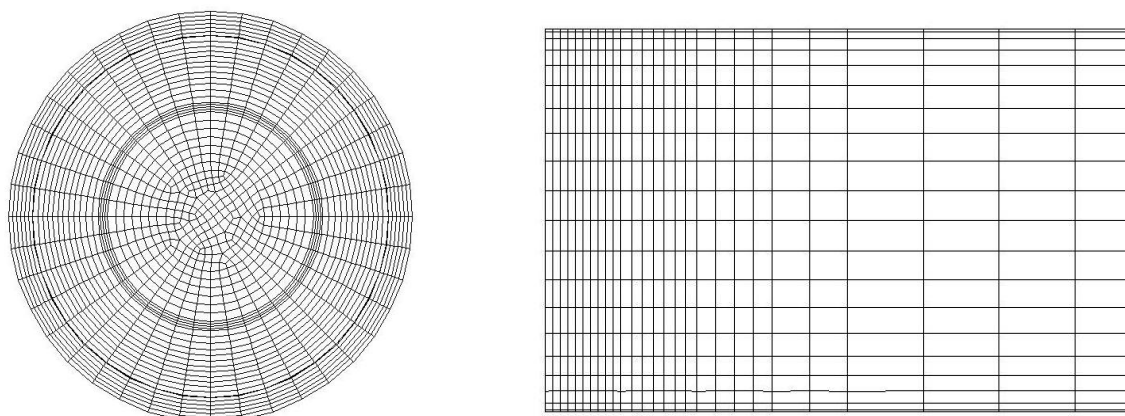


Fig. 2. Grid of burner cross-section (left) and a grid section nearby burner along the kiln (right).

- 1) The system is defined only from the burner tip onwards along the kiln (i.e. the real kiln was modified by shortening the length by 5m, therefore 63m kiln length was simulated instead of 68m).

B. Fuel and Gas Properties

The particle size distributions of coal and MBM are shown in Fig. 3.

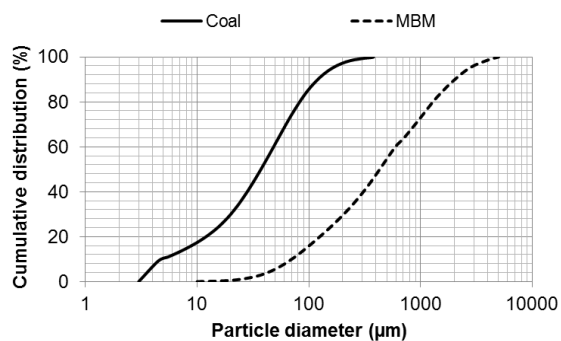


Fig. 3. Particle size distribution of coal and MBM [10].

Some of fuel properties are presented in Table I and gas properties are described in elsewhere [3], [10]. Default model parameters are used for the char combustion of both fuels [12]. The swelling coefficient is defined as 1.4 for coal and 1 for MBM. The particles are introduced as a number of uniform surface injections.

TABLE I: PROPERTIES OF FUELS (AS RECEIVED BASIS, UNLESS SPECIFIED)

Property	Coal	MBM
C (wt%)	72.9	47.1
H (wt%)	3.9	6.9
O (wt%)	5.6	4.5
S (wt%)	1.4	0.5
N (wt%)	1.7	9.7
Volatiles (wt%)	23.0	60.9
Fixed carbon (wt%)	62.4	8.0
Ash (wt%)	13.6	27.1
Moisture (wt%)	1.0	4.0
Higher heating value (HHV) (MJ/kg)	29.06	19.99
Lower heating value (LHV) (MJ/kg)	28.25	18.50
Dry particle density (kgm ⁻³)	1287 [14]	1354 [15]
Water-liquid fraction (vol%)	0.0131	0.056
Activation energy for devolatilization (J/mol)	7.4e4 [16]	1.7e5 [17]
Frequency factor for devolatilization (s ⁻¹)	3.8e5 [16]	8.3e11 [17]
Smallest particle diameter (µm)	3.75	10.5
Largest particle diameter (µm)	373	4500
Mass-weighted average particle diameter (µm)	53.8	793.9

C. Boundary Conditions

The air inlets are treated as velocity inlets and the outlet as a pressure outlet. Walls are adiabatic with no-slip conditions. The mass flow rates of air streams in real kiln system and calculated velocities are presented in Table II

TABLE II: MOMENTUM AND THERMAL CONDITIONS AT AIR INLETS AND GAS OUTLET

Boundary	Mass flow rate (kg/s)	Area (m ²)	Temp-erature (K)	Velocity (m/s)
Central tube for MBM	0.31	0.0104	323	28
Swirl air inlet	1.18	0.0074	323	Axial: 148 Tangential: 39
Fuel annulus for coal	0.73	0.0169	323	40
Jet air inlet	0.38	0.0008	323	459
Secondary air inlet	Case dependent	11.9190	1023	Case dependent
Pressure outlet	-	12.0663	-	-

Fuel-conveying air mass flow rates are fuel-type dependent (Table II). The secondary air mass flow rate is calculated in order to achieve 2 vol% of O₂ in the exhaust gas after complete combustion (Table II and Table III). The swirl number specific to the current burner is 0.261 and the

tangential velocity w at the swirl inlet is determined as follows.

$$w = Su \quad (16)$$

D. Solution Strategy and Convergence Criterion

The solution strategy is explained elsewhere [3], [10] and not repeated here. For the level of accuracy, the limited residual values for convergence are 10^{-3} for continuity and 10^{-4} for the other equations.

E. Case Definition

Four multi-fuel combustion cases were simulated. In all cases, the energy input to the kiln is 63.8 MW. The fuel temperature and velocity are similar to those of the air stream that conveys the fuel into the kiln (Table II and III). The case definition is summarized in Table III. In Table III, “central tube” and “annulus” in the feeding position column correspond to “Waste-derived solid fuel + air” and “Coal + air” inlets, respectively, in Fig. 1. The cases involve 10% (case 1), 32% (case 2), 59% (case 3) and 90% (case 4) primary coal energy replacement by MBM, respectively.

IV. RESULTS AND DISCUSSION

First, some general observations from the simulated results are presented and discussed. Second, the correlations between fuel replacement ratio and char burnout and temperature are compared. Finally, a limiting value for fuel replacement is suggested with respect to overall char burnout at the kiln inlet.

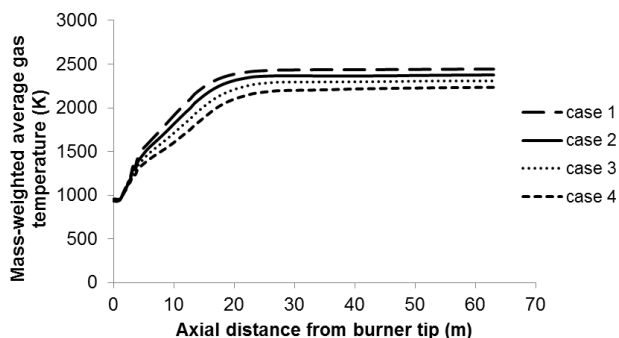


Fig. 4. Mass-weighted average gas temperature along the kiln.

A. General Impacts Due to Fuel Characteristics

Fig. 4 shows the mass-weighted average temperature (mass-averaged quantity over cross sections along different kiln axis locations) for four cases. The higher the replacement of coal by MBM, the lower is the equilibrium gas temperature. As long as the total energy supply to the kiln is constant, the lower temperature can be explained by; 1) increased exhaust gas flow due to higher air supply [7] and a higher amount of water vapour evaporated from fuel moisture, 2) higher fuel ash and moisture content, 3) poorer fuel burnout [18]. The energy-specific stoichiometric air demands for the four cases are 0.345, 0.360, 0.381 and 0.404 kg/MJ, respectively, resulting from the ultimate analysis and heating value of the fuel. It can be seen that when the replacement of MBM is higher, the air requirement is higher resulting in higher exhaust gas flow rates. The lower oxygen content (Table I)

and lower net calorific value (LHV) of MBM gives a higher air requirement, while the higher molar H/C ratio and lower sulphur content of MBM (Table I) gives a lower air requirement. In this case, the positive effect of the latter two factors is outweighed by the two former factors. The higher

ash and moisture content in MBM (Table I) also contribute to reduced temperature, since the ash and evaporated water vapour must be heated up to the equilibrium temperature [10].

TABLE III: SIMULATION CASES

Case	Fuel	Feeding position	Particle size distribution	Fuel feed rate (t/hr)	Fuel conveying air feed rate (kg/s)	Fuel conveying air velocity (m/s)	Secondary air mass flow rate (kg/s)	Secondary air velocity (m/s)
Case 1	MBM	central tube	MBM	1.242	0.309	28	21.76	5.35
	+coal	+annulus	+coal	+7.322	+0.727	+40		
Case 2	MBM	central tube	MBM	3.976	0.309	28	22.95	5.65
	+coal	+annulus	+coal	+5.532	+0.727	+40		
Case 3	MBM	central tube	MBM	7.330	0.309	28	24.50	6.03
	+coal	+annulus	+coal	+3.336	+0.727	+40		
Case 4	MBM	central tube	MBM	11.182	0.309	28	26.00	6.40
	+coal	+annulus	+coal	+0.814	+0.727	+40		

Table IV summarizes the devolatilization and char burnout percentages at the kiln end. The coal devolatilization is 100% and MBM devolatilization is in the range of 98-99%. Therefore, the overall devolatilization is 99-100% in all four cases. However, it can be seen in Table IV that the overall combusted char percentage at the kiln end is decreasing when the MBM percentage is increasing. This poor overall char burnout is mainly due to MBM char (Table IV). However, since the volatiles fraction in MBM is high, the highest overall unburnt char (18% in case 4) corresponds to only 3.5% of the total energy flow to the system. This corresponds to about 33K reduction in equilibrium gas temperature, i.e. not a huge impact.

TABLE IV: DEVOLATILIZATION AND CHAR BURNOUT AT THE KILN END

Case	Devolatilization at the kiln end (wt%)			Char burnout at the kiln end (wt%)		
	Coal	MBM	Overall	Coal	MBM	Overall
Case 1	100.0	99.1	99.7	100.0	84.4	99.6
Case 2	100.0	98.9	99.3	100.0	81.8	98.4
Case 3	100.0	98.7	98.9	100.0	77.7	95.0
Case 4	100.0	98.6	98.7	99.9	72.4	82.2

It can be concluded that the lower oxygen content and lower LHV and also the higher moisture and ash content of MBM have a significant impact on reducing temperature. In fact, these chemical characteristics of MBM are the main reasons for temperature reduction with increased replacement ratios, not poor fuel burnout. However, in a real cement kiln, the temperature decreases after the maximum point due to interaction with the solid raw materials and the non-uniform heat loss through the shell [19].

The results from devolatilization and char burnout are briefly discussed here, and one may find complementary information in previous publications for single fuel combustion [3], [10]. Fig. 5 shows the volatiles mass fraction contours for the four cases. The high volatiles mass fraction nearby the burner tip is mainly due to devolatilization. Intense devolatilization of MBM nearby the burner is due to the high volatiles content of MBM compared to coal (Table I). This is clearly shown in Fig. 5; a more pronounced effect can be observed with the increments of fuel replacement ratio. The different devolatilization kinetics of two fuels can also be a reason for different volatiles concentration profiles [3].

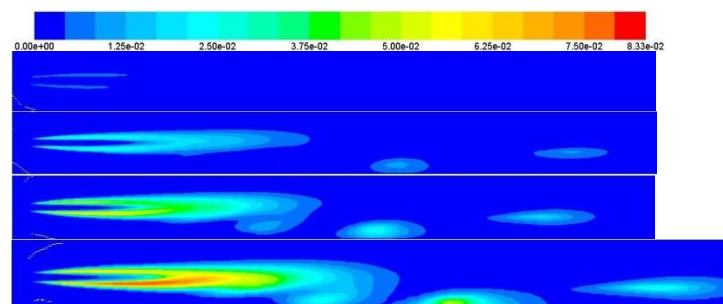
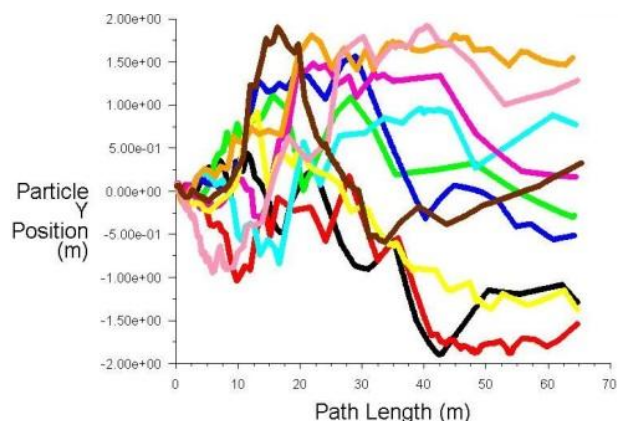
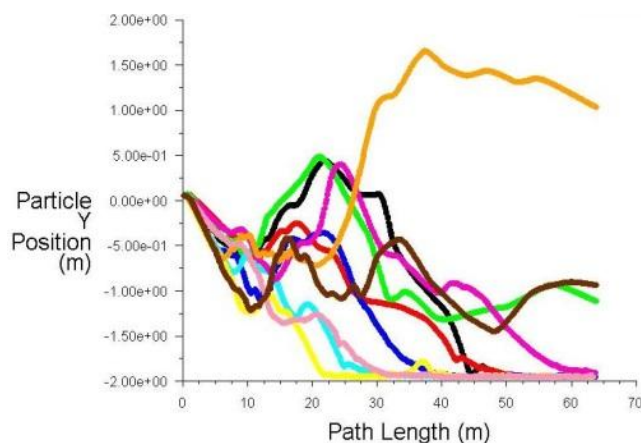


Fig. 5. Contours of volatiles mass fraction for cases 1, 2, 3 and 4, respectively (from burner tip to 38m).


 Fig. 6 (a). Particle tracks of ten random particles of diameter 12 μm ; case 4 (10 random particles have a different particle history due to stochastic tracking of particles.).

 Fig. 6 (b). Particle tracks of ten random particles of diameter 275 μm ; case 4 (10 random particles have a different particle history due to stochastic tracking of particles.).

The local high volatiles regions at the bottom of the kiln are significant when the coal replacement increases (Fig. 5). This can be explained by the fuel characteristics. The largest MBM particle diameter is 12 times bigger than the largest coal particle, and the mean particle diameter is 15 times bigger. The larger particle size of MBM compared to coal causes MBM particles to move downwards inside the kiln due to gravity forces (Fig. 6(a) and 6(b)). This effect is more prominent for MBM particles, since the MBM particle size distribution is in a wide range compared to coal. Therefore, the devolatilization of bigger particles continues at the lower part of the kiln producing more volatiles (Fig. 5).

As shown in Table IV, the overall char burnout percentage is reduced when coal replacement increases. Fig. 7 shows the maximum char burnout rate in different cross sections along the kiln. When the replacement ratio is the lowest, the char burnout is fastest at the beginning, and it is reduced consecutively with increasing replacement ratio. It can also be observed that char is burning along the kiln length when the replacement ratio is high. The reason for char burning areas continuing for a longer distance in the lower part of the kiln may be slower char burning. Slower char burning can be due to bigger particle size of MBM and hence lower particle temperature [3].

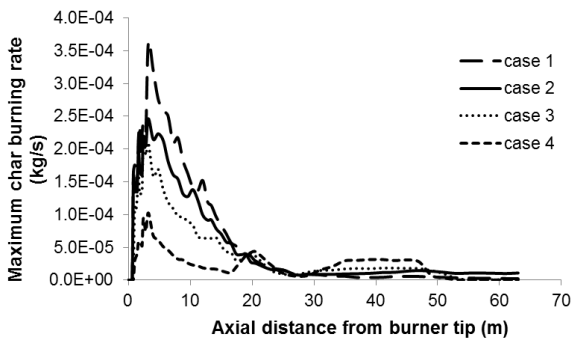


Fig. 7. Maximum char burning rate variations in different cross sections along the kiln.

B. Correlation of Fuel Replacement Ratio with Equilibrium Gas Temperature and Overall Char Burnout

A plot of mass-weighted equilibrium gas temperature as a function of coal replacement ratio is shown in Fig. 8. Downstream of around 50m of kiln axial position, the mass-weighted temperature was found to be nearly constant, therefore the average mass-weighted equilibrium gas temperature in the last 13m of the kiln is chosen for comparison.

The higher the replacement ratio the lower the equilibrium gas temperature, as is also shown in Fig. 4. The reasons for the temperature difference of 211 K from case 1 (10% replacement) to case 4 (90% replacement) is explained in section IV.A. Most importantly, it can be observed that the correlation between mass-weighted equilibrium gas temperature and fuel energy replacement ratio is more or less linear.

Fig. 9 shows the char burnout percentage at the kiln end for different replacement ratios. A linear correlation between the two end points (10 and 90 % replacement) is also plotted. It is clearly seen that the char burnout has a non-linear correlation with fuel replacement ratio. This can be explained by the non-linear relationship between temperature and char

burnout in the char combustion model and the radiation model.

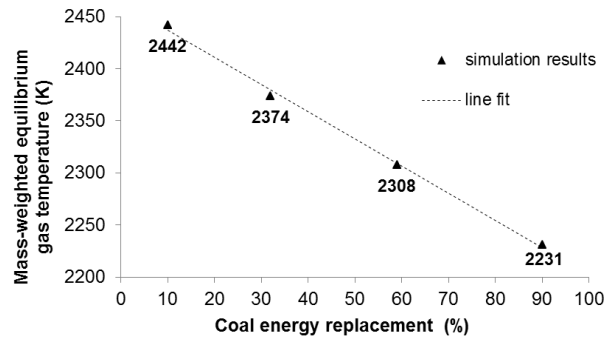


Fig. 8. Mass-weighted equilibrium gas temperature for different fuel replacement ratios.

Line AB in Fig. 9 indicates the maximum deviation between the two lines, i.e. up to this point, there is a relatively modest negative impact (reduction from 99.6% to 94.9%) on char burnout, whereas after this point, the negative impact on burnout accelerates (from 94.9% to 82.3%). Hence, the fuel replacement ratio corresponding to this point, about 58 %, could be taken as a maximum value which should not be exceeded, from a char burnout point of view.

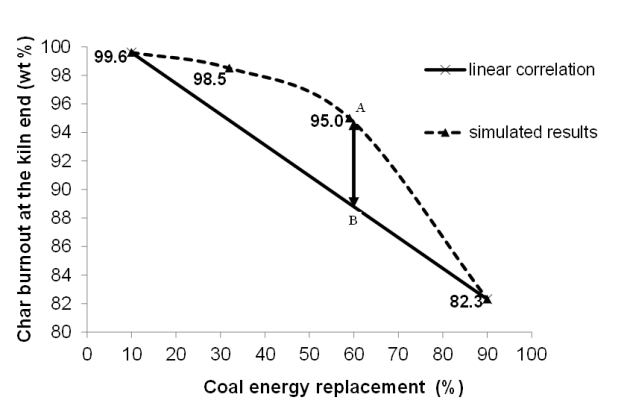


Fig. 9. The char burnout percentage at the kiln end for different fuel replacement ratios.

In a full-scale experiment carried out with a mixture of coal and MBM, it was found that there is an issue related to product quality when the replacement ratio exceeds about 50% [9], which was basically explained by a negative impact of reduced temperature. In the present study, it was found that the replacement ratio should be kept below about 58% in order to get maximum advantages of fuel replacement with respect to fuel char burnout point. A higher replacement ratio will readily result in a higher amount of unburnt fuel char, and this can negatively impact the internal cycles of sulphur, chlorine and alkalis in the kiln system as explained elsewhere [11]. Therefore, it can be concluded that a coal energy replacement ratio up to approximately 50% can be recommended in cement rotary kiln burners. Significantly higher replacement ratios should be avoided due to potentially negative impacts on the product and the process.

V. CONCLUSION

Multi-fuel combustion of coal and meat and bone meal (MBM) in a cement rotary kiln was simulated using a

commercial CFD software. The coal replacement ratios by MBM were 10%, 32%, 59% and 90% by energy.

The higher the replacement ratio, the lower the gas temperature. The equilibrium gas temperature difference between 10% and 90% replacement cases is around 211K. The reduction of temperature is due to lower net calorific value, lower oxygen content, high ash and moisture content and poor char burnout of MBM. Since MBM has a lower fixed carbon content, the effect from poor MBM char burnout contributes only to 1.4% reduction of the gas temperature. The rest of the chemical characteristics give the major contribution. It was also seen that devolatilization and char burnout are slower when the replacement ratio increases. This is basically due to the larger mean particle size of MBM which influence the particle temperature. These findings are compatible with simulation results previously published for single fuel combustion cases.

There is a linear correlation between gas temperature and fuel replacement ratio. But the correlation between overall char burnout and fuel replacement ratio is non-linear. To get the best out of this positive non-linearity, one should not exceed about 58% fuel replacement. Since the unburnt fuel char may disturb the internal cycles of sulphur, chlorine and alkalis in the cement kiln system, it is important to keep the unburnt fuel char level at a minimum.

NOMENCLATURE

a	absorption coefficient, m^{-1}
C	linear-anisotropic phase function coefficient
$C_{1\varepsilon}$	model constant, 1.42
$C_{3\varepsilon}$	model constant
$C_{2\varepsilon}^*$	model constant
E	total energy per unit mass, J/kg
\vec{F}	external body force vector per unit volume, N/m^3
F_D	drag force per unit mass and unit velocity, s^{-1}
G	incident radiation, W/m^2
G_b	generation of turbulence kinetic energy due to buoyancy, $J/(m^3 \cdot s)$
G_k	generation of turbulence kinetic energy due to the mean velocity gradients, $J/(m^3 \cdot s)$
\vec{g}	gravitational acceleration, m/s^2
h	enthalpy, J/kg
h_i	enthalpy of species i , J/kg
I	unit tensor
\vec{j}_i	diffusion flux of species i , $kg/(m^2 \cdot s)$
k	Turbulence kinetic energy per unit mass (J/kg)
k_{eff}	effective thermal conductivity, $W/(m \cdot K)$
n	refractive index
P	static pressure, Pa
q_r	radiation heat flux, W/m^2
R_i	net rate of production of species i by chemical reaction, $kg/(m^3 \cdot s)$
S	swirl number
S_h	heat of chemical reaction and any other volumetric heat source, W/m^3
S_i	rate of creation of specie i by addition from the dispersed phase, $kg/(m^3 \cdot s)$
S_m	mass added to the continuous phase from the dispersed second phase, $kg/(m^3 \cdot s)$
T	temperature, K

t	time, s
u	axial velocity, m/s
u_i	velocity magnitude in i^{th} direction, m/s
\vec{u}_p	particle velocity vector, m/s
\vec{u}	mean fluid phase velocity, m/s
\dot{u}	instantaneous value of the fluctuating gas flow velocity, m/s
v	velocity, m/s
\vec{v}	overall velocity vector, m/s
w	tangential velocity, m/s
x_i	distance in i^{th} direction, m
\vec{x}	overall distance vector, m
Y_i	mass fraction of species i

Greek letters

α_k	inverse effective Prandtl number for k
α_ε	inverse effective Prandtl number for ε
ε	dissipation rate of turbulence, m^2/s^3
μ_{eff}	effective dynamic viscosity, $Pa \cdot s$
ν_i	stoichiometric coefficients for reactants and products
ρ	density of continuous phase, kg/m^3
ρ_p	density of the particle, kg/m^3
σ	Stefan-Boltzmann constant, $5.67 \times 10^{-8} W/(m^2 \cdot K^4)$
σ_s	scattering coefficient, m^{-1}
$\bar{\tau}$	stress tensor, Pa
$\bar{\tau}_{eff}$	effective stress tensor, Pa
Γ	Diffusion coefficient in radiation, m

REFERENCES

- [1] F. Schorch, I. Kourti, B. M. Scalet, S. Roudier, and L. D. Sancho, *Best Available Techniques (BAT) Reference - Document for the Production of Cement, Lime and Magnesium Oxide*, 2013.
- [2] A. Rahman, M. G. Rasul, M. M. K. Khan, and S. Sharma, "Impact of alternative fuels on the cement manufacturing plant performance: An overview," *Procedia Engineering*, vol. 56, pp. 393-400, 2013.
- [3] W. K. H. Ariyaratne, A. Malagalage, M. C. Melaaen, and L.-A. Tokheim, "CFD modelling of meat and bone meal combustion in a cement rotary kiln – Investigation of fuel particle size and fuel feeding position impacts," *Chemical Engineering Science*, vol. 123, pp. 596-608, 2015.
- [4] T. Abbas, F. C. Lockwood, and S. S. Akhtar, "Plant performance improvement through "mathematical modelling," *ZKG International*, vol. 59, no. 12, pp. 49-60, 2006.
- [5] S. Suhail, T. Abbas, and F. C. Lockwood, "Advanced computational tools for cement plants," in *Proc. 2008 Cement Industry Technical Conference Record*, 2008.
- [6] P. Mtui, "CFD modeling of devolatilization and combustion of shredded tires and pine wood in rotary cement kilns," *American Journal of Energy Engineering*, vol. 1, no. 5, pp. 51-55, 2013.
- [7] U. Kääntee, R. Zevenhoven, R. Backman, and M. Hupa, "Cement manufacturing using alternative fuels and the advantages of process modelling," *Fuel Processing Technology*, vol. 85, no. 4, pp. 293-301, 2004.
- [8] W. K. H. Ariyaratne, E. V. P. J. Manjula, M. C. Melaaen, and L.-A. Tokheim, "Mathematical model for alternative Fuel combustion in a rotary cement kiln burner," *International Journal of Modeling and Optimization*, vol. 4, no. 1, pp. 56-61, 2014.
- [9] W. K. H. Ariyaratne, M. C. Melaaen, K. Eine, and L. A. Tokheim, "Meat and bone meal as a renewable energy source in cement kilns: Investigation of optimum feeding rate," presented at the International Conference on Renewable Energies and Power Quality, Las Palmas de Gran Canaria (Spain), 2010.
- [10] W. K. H. Ariyaratne, A. Malagalage, M. C. Melaaen, and L.-A. Tokheim, "CFD modeling of meat and bone meal combustion in a

rotary cement kiln," *International Journal of Modeling and Optimization*, vol. 4, no. 4, pp. 263-272, 2014.

- [11] L. A. Tokheim, "The impact of staged combustion on the operation of a precalciner cement kiln," PhD Thesis, Telemark College, Norway, 1999.
- [12] Fluent, "Discrete phase," *Ansys Fluent Theory Guide 130*, USA: Ansys Inc, 2010, pp. 367-454.
- [13] B. F. Magnussen and B. H. Hjertager, "On mathematical modeling of turbulent combustion with special emphasis on soot formation and combustion," in *Proc. Symposium (International) on Combustion*, vol. 16, no. 1, pp. 719-729, 1977.
- [14] O. P. Mahajan and P. L. Walker, "Porosity of coals and coal products," *Analytical Methods for Coal and Coal Products*, vol. 1, USA: Academic Press, Inc, 1978.
- [15] R. A. Garcia, K. A. Rosentrater, and R. A. Flores, "Characteristics of North American meat and bone meal relevant to the development of non-feed applications," *Applied Engineering in Agriculture*, vol. 22, no. 5, pp. 729-736, 2006.
- [16] S. Badzioch, and P. G. W. Hawksley, "Kinetics of thermal decomposition of pulverized coal particles," *Industrial & Engineering Chemistry Process Design and Development*, vol. 9, no. 4, pp. 521-530, 1970.
- [17] G. Skodras *et al.*, "A kinetic study on the devolatilisation of animal derived byproducts," *Fuel Processing Technology*, vol. 88, no. 8, pp. 787-794, 2007.
- [18] W. K. H. Ariyaratne, "Utilization of waste-derived biofuels and partly CO₂ neutral fuels in cement kilns," PhD thesis, Telemark University College, Norway, 2014.
- [19] S. Wang, J. Lu, W. Li, J. Li, and Z. Hu, "Modelling of pulverised coal combustion in cement rotary kiln," *Energy and Fuels*, vol. 20, pp. 2350-2356, 2006.



W. K. Hiromi Ariyaratne received her PhD degree in combustion (Telemark University College (TUC), Porsgrunn, Norway, 2014) and one MSc degree in process technology (TUC, 2009) and another MSc degree in chemical and process engineering (University of Moratuwa (UOM), Moratuwa, Sri Lanka, 2007) and a BSc degree in chemical and process engineering (UOM, 2004).

She is postdoctoral fellow at TUC since 2014, where her topic is related to CFD modeling of pneumatic conveying of drill cuttings. She has worked on research projects as a research fellow in Sevanagala Sugar Industries (Pvt) Ltd, Sri Lanka and Research and Development Institute, Sri Lanka (2006-2007). She has work experience as chemical and process engineer in Hammer International (Pvt) Ltd, Sri Lanka (2006) and Linea Intimo (Pvt) Ltd, Sri Lanka (2003). She has also worked at Department of Chemical and Process Engineering at UOM (2005).

Dr. Ariyaratne's research interests are alternative fuel combustion in cement clinker production, pneumatic conveying, modeling and simulation, fluid dynamics, heat and mass transfer, cleaner production and waste management techniques.



Morten C. Melaaen received his MSc degree in mechanical engineering in 1986 and his PhD in 1990, both from Norwegian University of Science and Technology (NTNU), Trondheim, Norway.

He is a professor in process technology at Telemark University College, Porsgrunn, Norway. He is also the dean of Faculty of Technology, Telemark University College and has a part time position at the local research institute Tel-Tek. Earlier, he has worked as a Research Engineer in Division of Applied Thermodynamics, SINTEF, Norway and as an Associate Professor at NTNU. He has worked on research projects as a Senior Research Scientist in Norsk Hydro Research Centre Porsgrunn, Norway. He started to work as a professor at Telemark University College in 1994 and became Head of Department, Department of Process, Energy and Environmental Technology in 2002.

Prof. Melaaen's research interests are CO₂ capture, modeling and simulation, fluid mechanics and heat and mass transfer. Prof. Melaaen has more than 110 scientific papers published in the above mentioned related fields in international journals and conferences.



Lars-André Tokheim has a PhD degree in combustion (Telemark University College (TUC), Porsgrunn, Norway, 1999), an MSc degree in industrial environmental technology (TUC, 1994) and a BSc degree in chemistry (TUC, 1992).

He is an associate professor at TUC since 2006, where he teaches gas purification and heat & mass transfer, supervises MSc and PhD students, and coordinates master study programmes in Process Technology and Energy & Environmental Technology as well as a PhD study programme in process, energy & automation engineering. He has industrial experience from Norcem/HeidelbergCement since 1994: as a Research Scholar (1994-1998), as a process engineer in the Production Department (1998-2001), and as the head of Department for Process Development and Environment (2001-2006).

Prof. Tokheim's main research interests include use of alternative fuels in cement clinker production, calciner technology and gas pollution reduction, in particular CO₂ capture and NO_x reduction.